

AD-A098 193

KANSAS STATE UNIV MANHATTAN DEPT OF PHYSICS

F/G 20/2

PULSED RAMAN TEMPERATURE MEASUREMENTS OF LASER-HEATED SILICON (U)

1980 A COMPAAN: H W LO

N00014-80-C-0419

UNCLASSIFIED

NL

1-1  
AD-A098 193



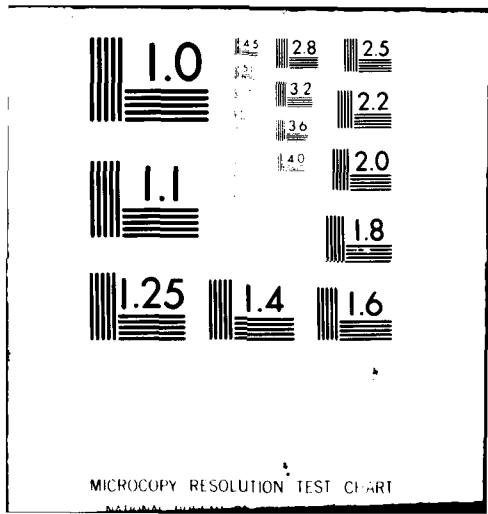
END

DATE

FILMED

5-81

DTIC



MICROCOPY RESOLUTION TEST CHART

to appear in Proceedings of the 11th Int'l Conf. on Defects and Radiation Effects in Semiconductors, Oiso, Japan, Sept 8-11, 1980 (Inst. Phys. Conf. Ser.)

PULSED RAMAN TEMPERATURE MEASUREMENTS OF LASER-HEATED SILICON

10 Compaan ~~and~~ H, W, Lo

12 (15) NA0014-1A-1-0419

Department of Physics, Kansas State University, Manhattan, KS, 66506

12

ABSTRACT

Time resolved Raman light scattering determinations of temperature have been made in crystalline silicon where it is found that the lattice temperature is far below melting even for laser power densities of  $\sim 1 \text{ J/cm}^2$  at 485 nm. In ion-implantation-amorphized silicon the pulsed laser Raman technique has identified substantial recrystallization as early as 30 nsec after the peak of the heating pulse.

1. Introduction

Pulsed laser and electron beam annealing of ion-implantation-produced damage in semiconductors is fast becoming a valuable tool in semiconductor processing. Laser annealed specimens have been thoroughly studied with a great variety of probes, (Khaibullin 1978, and Brown 1980) usually hours, to days after the pulsed anneal and the results used to construct scenarios of the pulsed anneal process itself. However, there is a distinct lack of direct data on conditions prevailing in the semiconductor during the anneal process. The notable exception is the use of time-resolved reflectivity by Auston, et al (1978) and subsequently by several other groups. We have recently demonstrated that Raman scattering can be used with nanosecond time resolution to probe the temperature of laser-heated crystalline silicon. We review here the results of these temperature measurements and in addition present Raman results obtained from ion-implanted silicon.

2. Theory

The temperature measurements were obtained from the ratio of Stokes to anti-Stokes scattering from the  $520 \text{ cm}^{-1} \Gamma_{25+}$  phonon Raman line in crystalline silicon. The ratio of Stokes to anti-Stokes counting rates is given by

$$\frac{R_S}{R_{AS}} = \frac{(\alpha_L + \alpha_{AS}) \omega_S^3 \sigma(\omega_L, \omega_S)}{(\alpha_L + \alpha_S) \omega_{AS}^3 \sigma'(\omega_L, \omega_{AS})} e^{\hbar\omega_0/kT} \quad (1)$$

where  $\omega_L$ ,  $\omega_S$ ,  $\omega_{AS}$  and  $\omega_0$  are the laser, Stokes, anti-Stokes and phonon frequencies respectively.  $\sigma(\omega_L, \omega_S)$  and  $\sigma'(\omega_L, \omega_{AS})$  are the Stokes and anti-Stokes Raman scattering cross sections and the term  $\exp(\hbar\omega_0/kT)$  follows directly from the ratio  $[n(\omega_0) + 1]/n(\omega_0)$  where  $n(\omega_0)$  is the phonon occupation probability at the lattice temperature  $T$ . For Raman scattering with laser frequencies above the band gap in semiconductors it is essential to include the frequency dependence of the cross sections  $\sigma$  and  $\sigma'$  and furthermore to correct for the reduced scattering volume due to strong absorption of the laser and scattered beams. These corrections are known or can be measured and are discussed more fully

LEVEL II

DTIC ELECTRIC  
APR 24 1981  
S

DISTRIBUTION STATEMENT A  
Approved for public release;  
Distribution Unlimited

AD A 098193

DTIC FILE COPY

81 3 05 053

by Lo (1980). In addition the intensity ratios have been corrected for differences in spectrometer and detector efficiency at the Stokes and anti-Stokes frequencies.

### 3. Experimental

#### 3.1 Apparatus

The data on crystalline silicon were obtained with a Spex 1401 double spectrometer and an ITT FW 130 photomultiplier used in a gated photon counting mode. Since the crystalline silicon was observed to damage after repeated ( $10^2$ - $10^4$ ) pulses at focussed energy densities near  $1 \text{ J/cm}^2$ , a low speed synchronous motor (4 RPM) was used to rotate the sample. The motor was occasionally translated so that the pulsed beam swept out a pattern roughly like a needle on a phonograph record.

The ion-implanted silicon samples were obtained from Spire Corporation implanted with 200 keV arsenic to a dose of  $10^{15}/\text{cm}^2$ . This dose is sufficient to amorphize a layer roughly 150 nm thick. For this data an X-Y scanning stage was used to raster scan the sample so that each laser pulse impacted on virgin unannealed surface material. A PDP 11/34 computer was used to control the scan pattern and also to control a PARC OMA-2 vidicon with a 1254 SIT detector head, which was used for data acquisition. This multichannel detector replaced the photomultiplier at the output of the Spex 1401. The OMA-2 was cooled to dry ice temperature and signal was typically integrated for 10 minutes. During readout 10 adjacent channels were integrated before digitizing and then sent to the computer for storage and background subtraction. The effective detector resolution was therefore 250  $\mu\text{m}$ ; however the image size of  $\sim 700 \mu\text{m}$  at the entrance slit was the resolution-limiting factor. To reduce stray light the intermediate slit was typically operated at 1000  $\mu\text{m}$ .

#### 3.2 The Heat/Probe Technique

Lattice temperatures may in principle be obtained from the Raman scattered light of the heating or annealing laser pulse itself. However, in this case the Stokes-anti-Stokes ratios would average over the rising lattice temperature during the heating pulse. Furthermore, spatial variations in the power density would be reflected in spatial temperature variations so that the fringes of the beam would presumably sample a much lower lattice temperature than the beam center. Finally, the exponential attenuation of laser intensity into the crystal would produce a strong temperature gradient that would be reflected in the Raman signal. To minimize these three averaging effects we chose to use a two-beam configuration with an intense heating beam and a weak, delayed probe beam. In addition the probe was focussed to a diameter at half power points approximately 1/3 to 1/2 that of the heating beam which was typically 200  $\mu\text{m}$ . Spot overlap was repeatedly checked with a 50  $\mu\text{m}$  pinhole placed at the exact position of the silicon sample. The use of a probe beam also allowed us to select a shorter wavelength ( $\lambda_P = 406.5 \text{ nm}$ ) which is more strongly absorbed in crystalline silicon ( $\alpha = 6 \times 10^4 \text{ cm}^{-1}$ ) than the heating laser wavelength ( $\lambda_H = 485 \text{ nm}$ ) where  $\alpha = 1.2 \times 10^4 \text{ cm}^{-1}$ . A Molelectron UV-1000 pulsed nitrogen laser was used

to excite simultaneously the two dye lasers. Maximum power for the heating pulse was obtained from a broad-band dye laser ( $\Delta\lambda \approx 10$  nm) with no dispersive element in the cavity while the probe pulse was obtained from a Molelectron DL-200 dye laser. A confocal spherical-mirror optical delay line was used to obtain the variable delays for the probe pulse.

#### 4. Temperature Measurements in Crystalline Silicon

The lattice temperature rise in crystalline silicon as a function of heating laser power density is shown in Fig. 1. The first point was taken with the heating beam blocked; it indicates the presence of some heating due to the probe pulse. However, the need to focus the probe to  $\sim 50$   $\mu\text{m}$  made data acquisition at lower probe power densities very difficult. Note that the average probe power at the 15 pulse-per-second repetition rate was typically 60 microwatts. To check for non-linear effects due to heating from the probe beam, data were obtained at a probe power density of  $0.2$   $\text{J}/\text{cm}^2$  in addition to the  $0.06$   $\text{J}/\text{cm}^2$  shown in Fig. 1. The results indicated  $\sim 80^\circ\text{C}$  greater lattice heating from the probe but otherwise were qualitatively similar to the results shown in Fig. 1. The power densities indicated in Fig. 1 represent the power density at the center of the heating beam. They were obtained with a  $50$   $\mu\text{m}$  pinhole positioned at the center of each focussed spot and average power was determined by a Scientech disk

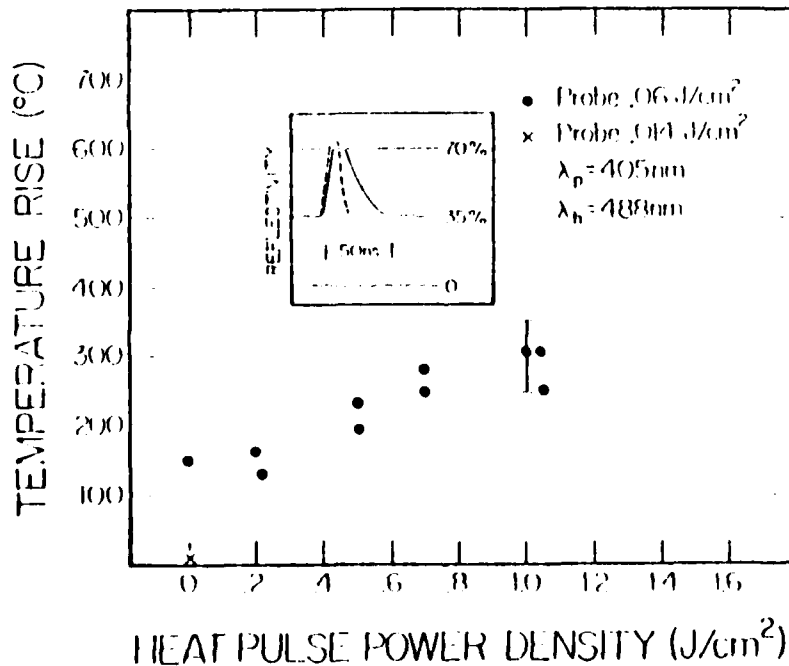


Figure 1. Temperature rise of crystalline silicon measured 10 nsec after a 7 nsec heating pulse. Inset shows shape of heat pulse (dotted line) and the reflectivity rise at 633 nm (solid line).

Accession For	
NTIS GRA&I	<input checked="" type="checkbox"/>
DTIC TAB	<input checked="" type="checkbox"/>
Unannounced	
Justification	for file
By	sta/4/1/1/81
Distribution/	
Availability Codes	
Dist	Avail and/or Special
A	

calorimeter. The probe spot (50  $\mu\text{m}$  at half power points) was centered in the 90  $\mu\text{m}$  diameter spot of the heating beam. Pulse-to-pulse fluctuation of the intensities were  $\leq 5\%$ . The lattice temperature rise of only 300 $^{\circ}\text{C}$  for power densities of  $\approx 1 \text{ J/cm}^2$  indicates clearly that the silicon lattice is far from melting. However this data was obtained for a 10 nsec delay when our reflectivity measurement (see the inset of Fig. 1) showed the sample to be in the high reflectivity phase usually associated with melting. We believe therefore that the Raman data show unequivocally that this high reflectivity period is not due to a metallic transition associated with melting. If, in fact, the reflectivity jump indicated melting, then a dramatic drop in Raman signal should be observed at power levels sufficient to produce the reflectivity enhancement. (Molten silicon has no similar Raman line.)

An important feature of Raman measurements of temperature is that in the presence of temperature inhomogeneities the method contains a natural bias towards the higher temperature regions. For example, in silicon at 300 $^{\circ}\text{C}$  the phonon occupation factor is  $n = [\exp(\hbar\omega_0/kT) - 1]^{-1} = 0.37$ . Thus the Stokes signal (proportional to  $n + 1$ ) increases rather slowly with temperature but the anti-Stokes signal (proportional to  $n$ ) increases rapidly with temperature in this range. The result for an integrated signal is weighted toward the high temperature regions.

#### 5. Raman Signature of Recrystallization in Amorphized Silicon

The only evidence to date of the time scale on which recrystallization occurs after pulsed laser irradiation has been the fall of the reflectivity enhancement with the accompanying assumption that the high reflectivity is due to molten silicon. As discussed above, the Raman evidence shows this assumption to be incorrect. Raman scattering, however, allows one to time-resolve the recrystallization. The key to the success of the Raman measurement is the fact that amorphous silicon has no sharp Raman features and compared with the 520  $\text{cm}^{-1}$  mode of crystalline material,  $\alpha$ -silicon appears nearly Raman silent.

The onset of recrystallization in the ion-implanted amorphized silicon samples was studied using a variety of time delays with the 2.55 meter optical delay line. Figure 2 displays Raman signals obtained at probe delays of 28 nsec, 59 nsec, 212 nsec, and one spectrum taken with the heat beam off. The heating and probe power densities were 0.56  $\text{J/cm}^2$  and 0.11  $\text{J/cm}^2$  respectively, averaged over the central 50  $\mu\text{m}$ . One clearly sees the growth of the Raman signal is very rapid. The crystalline signal is essentially full size at 59 nsec and a sizeable signal occurs at 28 nsec. For comparison we display in the inset the shape of the reflectivity rise observed in this material with a 514.5 nm beam focussed to  $\approx 40 \mu\text{m}$  diameter at the center of the pulsed beams. Comparison with the trace of the two pulsed beams at 28 nsec delay shows that for some of the duration of the probe pulse the sample is in an enhanced reflectivity state.

To determine whether a Raman signal was in fact observable during the peak of the high reflectivity phase, we repeated the 28 nsec measurement using a power density of .87  $\text{J/cm}^2$  for the heating pulse. This produced a high reflectivity phase lasting a full 50 nsec followed by

a  $\sim 25$  nsec tail. The Raman signal was clearly present at a level of  $\sim 500$  counts in 5 minutes. These results further confirm that the reflectivity rise is not due to lattice melting since a molten phase has no well defined  $520 \text{ cm}^{-1}$  lattice mode.

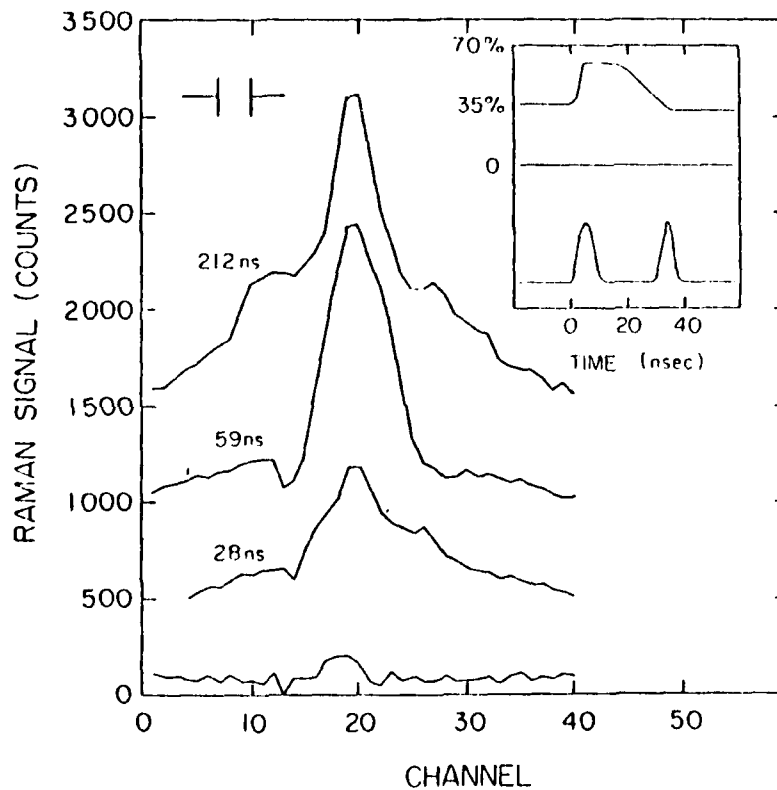


Figure 2. Stokes Raman spectrum of laser-annealed ion-implanted silicon obtained for various delays of the 406.5 nm probe pulse. For clarity successive traces are displaced vertically by 500 counts. The lowest trace was taken with the probe pulse only. Insets show 514 nm reflectivity and pulse timing at 28 nsec delay. Instrumental resolution of 3 channels is indicated; frequency shift calibration is  $8 \text{ cm}^{-1}/\text{channel}$ .

## 6. Discussion

We believe that a plausible explanation of the enhanced reflectivity phase is that it results from a high density electron-hole plasma in the solid state. It should be recalled that the light absorption mechanism at 488 nm in silicon is the creation of energetic electron-hole pairs. Normally, i.e. at low densities, electron-phonon and hole-phonon scattering rates are very rapid - of the order of  $10^{12} \text{ sec}^{-1}$  so that most of the excess carrier energy should be transferred to the

lattice in times of the order of nanoseconds. However, if one assumes for the purpose of argument, little carrier recombination and little carrier diffusion during the heating laser pulse, then the 485 nm heating pulse will generate an electron-hole pair density of  $1.7 \times 10^{22}/\text{cm}^3$  near the surface. This is considerably above the conduction band carrier density required to produce a metallic-like reflectivity at 514 nm in silicon. It is therefore crucial to understand the mechanisms by which carrier relaxation may be slowed under high density conditions. Van Vechten (1979, 1980a, 1980b) and Yoffa (1980) have already pointed out some interactions which may be important. We believe such processes must be explored further.

\* Supported by ONR Contract N00014-80-C-0419

#### References

1. Auston D H, Surko C M, Venkatesan T N C, Slusher R E and Golovchenko J A 1978 Appl. Phys. Lett. 33 437
2. Brown W L 1980 in Laser and Electron Beam Processing of Materials edited by C W White and P S Peercy Academic Press p. 20
3. Khaibullin I B, Shtyrkov E I, Zaripov M M, Bayazitov R M and Galjautdinov M F 1978 Radiation Effects 36 225
4. Lo H W and Compaan A 1980 Phys. Rev. Lett. 44 1604
5. Van Vechten J A, Tsu R, Saris F W and Hoonhout D 1979 Phys. Lett. 74A 417  
Van Vechten J A 1980a J. Phys. (Paris) 41 C4-15  
Van Vechten J A and Wautelet M 1980b this conference, paper F-3
6. Yoffa E J 1980 Phys. Rev. B 21 2415